Am. J. Trop. Med. Hyg., 97(5), 2017, pp. 1469–1476
doi:10.4269/ajtmh.17-0044

Benznidazole Nanoformulates: A Chance to Improve Therapeutics for Chagas Disease

Teresa Vinuesa,[1]* Rocio Herráez,[1] Laura Oliver,[1] Elisa Elizondo,[2] Argia Acarregui,[3] Amaia Esquisabel,[3] Jose Luis Pedraz,[3] Nora Ventosa,[2] Jaume Veciana,[2] and Miguel Viñas[1]

[1]*Department of Pathology and Experimental Therapeutics, Medical School, University of Barcelona, Barcelona, Spain;* [2]*Ciber-BBN (Nanomol), Department of Molecular Nanoscience and Organic Materials, Institut de Ciència de Materials de Barcelona (ICMAB-CSIC), Cerdanyola del Vallès, Spain;* [3]*Ciber-BBN (NanoBioCel), Laboratory of Pharmaceutics, School of Pharmacy, University of the Basque Country (UPV/EHU), Vitoria, Spain*

Abstract. This article describes the characterization of various encapsulated formulations of benznidazole, the current first-line drug for the treatment of Chagas disease. Given the adverse effects of benznidazole, safer formulations of this drug have a great interest. In fact, treatment of Chagas disease with benznidazole has to be discontinued in as much as 20% of cases due to side effects. Furthermore, modification of delivery and formulations could have potential effects on the emergence of drug resistance. The trypanocidal activity of new nanostructured formulations of benznidazole to eliminate *Trypanosoma cruzi* was studied in vitro as well as their toxicity in two cultured mammalian cell lines (HepG2 and Fibroblasts). Nanoparticles tested included nanostructured lipid carriers, solid lipid nanoparticles, liposomes, quatsomes, and cyclodextrins. The in vitro cytotoxicity of cyclodextrins–benznidazole complexes was significantly lower than that of free benznidazole, whereas their trypanocidal activity was not hampered. These results suggest that nanostructured particles may offer improved therapeutics for Chagas disease.

INTRODUCTION

Infection by *Trypanosoma cruzi* causes Chagas disease (American trypanosomiasis), a chronic systemic condition considered by the World Health Organization (WHO) a neglected tropical disease. The infection affects 6–8 million people worldwide and is the largest parasitic disease burden throughout the Americas.[1] Although previously confined to rural areas in Central and South America, it has now spread into urban zones in Latin America, North America, Europe, and even Japan.[2,3] The migration of chronically infected and asymptomatic individuals has led to the globalization of the disease. Moreover, its vectorial transmission by kissing bugs is no longer the unique mode of transmission. Rather nonvectorial infection, including vertical transmission, bloodborne, and intake of contaminated drinks has been reported, leading to an increase in the number of new cases and drastic changes in the classical epidemiology map of Chagas disease.[4,5]

The disease is characterized by a complex pathology involving the invasion and successful intracellular establishment of *T. cruzi* in certain tissues, including cardiac and skeletal muscle and the nerve cells of the heart and gastrointestinal tract.[6] The clinical course can be divided into three phases: 1) The early acute phase, when parasitemia can be detected, lacks specific symptoms and the majority of patients resolve spontaneously; however, this phase can be life-threatening in children or if myocarditis develops; 2) the disease progress to a silent, asymptomatic indeterminate phase in which parasites hide in different tissues; and with further progression 3) the clinical course evolves to a chronic phase. In 30% of the patients with chronic Chagas disease cardiomyopathy, megaesophagus, megacardias, or megacolon will develop. Thus, the disease remains a leading cause of cardiac mortality and gastrointestinal tract pathology. Treatment during the acute phase provides high cure rates, but the efficacy of drug therapy declines with increasing duration of the infection. Nevertheless, based on strong evidence of parasitic persistence as the cause of disease progression,[7] the WHO recommends that all adult patients with chronic Chagas disease should be treated.[8] Current therapeutic options include two nitro heterocyclic compounds, benznidazole (BNZ) and nifurtimox, empirically developed more than four decades ago.[9] Since 1980, the WHO has listed BNZ as a recommended drug for adults and children. However, although it is still considered the best treatment and has fewer side effects than nifurtimox, the cure rates achieved with BNZ in chronic-phase patients are low; it significantly reduces the parasitemia but there is no cardiomyopathy improvement.[10] Furthermore, the toxic profile of BNZ in adults is such that nearly 20% of patients must discontinue treatment because of hypersensitivity-related drug toxicity events[11] including dermatological, hematological, digestive, articular, and neurological ones, mostly appearing in the first 2 weeks.[12] Cutaneous side effects are the most common, although rates vary among series (18–56%). They are normally mild to moderate and manageable with antihistamines together with topical or low-dose systemic corticosteroids, although reports of severe skin reactions with possible atypical clinical findings have been published recently.[13] Based on these findings, the need for effective, but less toxic drugs is clear since in the absence of a vaccine, the control of the vector and the treatment of patients are the only available tools to fight the disease. Different strategies are being sought to overcome the toxicity of BNZ including shorter or intermittent administration schedules, either alone or in combination with other drugs.[14] Combinations have included the use of BNZ with ergosterol inhibitors although no additional benefits were seen when compared with monotherapy.[15,16] Another approach was to formulate the drugs to specifically target the affected tissues,[17] thus improving their bioavailability and by reducing the required dose, decreasing their toxicity. The targeting of drugs against *T. cruzi* using colloidal systems (e.g., liposomes [LPs] and nanoparticles) has been examined in several studies.[18–22] The low water solubility of BNZ (0.4 mg/mL) has been circumvented with different strategies, for example, using chitosan microparticles,[23] or solid dispersions in sodium

* Address correspondence to Teresa Vinuesa, Molecular Microbiology and Antimicrobials Laboratory, Medical School, University of Barcelona, Feixa Llarga s/n 08907 Hospitalet LLobregat Barcelona, Spain. E-mail: tvinuesa@ub.edu

TABLE 1
Description of the different types of SUVs (small unilamellar vesicles) investigated in the present work

Type of vesicle	Name	Composition*	Molar ratio of components	Lipid concentration (mg/mL)†
Quatsomes	QSa	Chol:MKC	1:1	5.5
	QSb	Chol:MKC:Chol_PEG	6:7:1	6.1
	QSc	Chol:BKC	1:1	5.7
	QSd	Chol:BKC	0.5:1	4.2
Liposomes	LPa	Chol:DPPC	1:1	1.4
	LPb	Chol:DPPC	0.72:1	5.2
	LPc	Chol:DPPC:Chol_PEG	6:9:1	1.4

SUV = small unilamellar vesicle.
* Membrane components of the SUVs. BKC = benzalkonium chloride; Chol = cholesterol; Chol-PEG = cholesterol functionalized with polyethyleneglycol (PEG1000); MKC = myristalkonium.
† Lipid concentration: total mass of membrane components comprising the SUVs divided by the total volume of vesicular suspension.

deoxycholate.[24] Cyclodextrins (CDs), a family of ring compounds made up of sugar molecules, are widely used in the pharmaceutical industry to improve solubility and oral bioavailability while diminishing toxicity. Their use in obtaining complexes of different drugs with trypanocidal action has been explored.[25–29]

The aims of the present work were 1) to determine the in vitro trypanocidal activity of new nanostructured formulations of BNZ:small unilamellar vesicles (SUVs) (conventional nanoLPs and quatsomes [QS], lipid nanoparticles [solid lipid nanoparticles (SLNs) and nanostructured lipid carriers (NLCs)]) and nanostructured CD complexes; and 2) to explore the toxicity of these agents in two cultured mammal cell lines.

MATERIALS AND METHODS

Cultures. *Trypanosoma cruzi* was grown axenically at 28°C in liver infusion–tryptose medium (LIT; Difco™ BD, MD; Pronadisa, Madrid, Spain) containing 10% fetal bovine serum (FBS; Gibco, Life Technologies, NY) plus antibiotics (100 μg/mL streptomycin + 100 U/mL penicillin G; Sigma-Aldrich, St. Louis, MO). Strains were maintained in exponential growth by weekly passages.[24] Tissue-culture-derived (TCD) trypomastigotes were obtained as follows: Murine L-929 fibroblasts were cultured in plastic tissue culture flasks (75 cm^2; VWR Int LLC, Radnor, PA) containing MEMHSP (minimal essential medium [MEM; Biochrom AG, Berlin, Germany] with Hepes [Sigma-Aldrich] plus antibiotics [SP]) until they formed a non-confluent monolayer. The cells were then infected with epimastigotes in the stationary phase of growth (14-day-old cultures), incubated for 24 hours in a humidified 5% CO_2 atmosphere at 33°C, and then washed with phosphate-buffered saline (AMRESCO, Solon, OH) to remove noninternalized parasites, incubation was in MEMHSP for 7–20 days, until a large number of free trypomastigotes appeared, they were then harvested by centrifugation.

The cytotoxicity[30] was determined in murine L-929 fibroblasts (NCTC clone 929, ECACC 88102702) and human hepatocellular carcinoma cell line Hep G2 (American Type Culture Collection [ATCC]).[31,32]

Drugs and nanoformulates. BNZ (Laboratorios ELEA, Buenos Aires, Argentina). Dipalmitoylphosphatidylcholine (DPPC) and cholesterol_PEG1000 (Chol_PEG) (Corden Pharma, Plankstadt, Germany); Hidroxy-propyl-β-CD (HP-β-CD) kindly given by Ashland Inc. (Barcelona, Spain); cholesterol (Chol) (AppliChem, Darmstadt, Germany); and surfactants, myristalkonium chloride and benzalkonium chloride (Sigma-Aldrich and Tres Cantos, Madrid, Spain) were used.

Four types of quatsomes (QS) and three of LP were prepared by a one-step procedure based on the use of compressed CO_2.[33] Ethanol and nonencapsulated BNZ were removed by diafiltration of nanovesicular suspensions. CDs loaded with BNZ were prepared by an antisolvent precipitation with compressed CO_2.[34] SLNs and NLCs were prepared as previously described.[35,36] Trehalose (15%), a well-known cryoprotectant, was used in the freeze-drying of the nanoparticles.

Cytotoxicity test. Cytotoxicity was determined by measuring the extracellular reduction of tetrazolium salts (water-soluble tetrazolium [WST]) (Roche, Pleasanton, CA).[37,38] The assay was

TABLE 2
Physicochemical characteristics (drug content, size, *Z*-potential, and morphology) of the different samples of SUVs

Name	Drug (%)*	Size (diameter)† Mean (nm)	Size (diameter)† PDI	*Z*-potential† (mV)	Morphology‡
QSa 0	0	115 ± 31	0.292 ± 0.001	+95.2 ± 1.4	Spherical: unilamellar and multivesicular
QSb 0	0	46 ± 13	0.304 ± 0.005	+94.4 ± 6.6	Spherical: unilamellar
QSc 0	0	124 ± 40	0.409 ± 0.031	+77.2 ± 0.4	Spherical: unilamellar (+fraction of non-vesicular phase)
QSd 0	0	104 ± 28	0.284 ± 0.005	+66.3 ± 0.6	Spherical: uni- and bilamellar
LPa 0	0	115 ± 23	0.167 ± 0.007	–12.1 ± 0.6	Spherical: uni- and multilamellar
LPb 0	0	122 ± 27	0.197 ± 0.007	–17.8 ± 0.5	Uni- and multilamellar
LPc 0 (1)	0	103 ± 25	0.230 ± 0.010	–15.3 ± 0.8	Unilamellar and non-assembled phospholipid bilayers
LPc 0 (2)	0	117 ± 47	0.235 ± 0.003	+21.1 ± 0.5	Spherical: unilamellar
LPb 0.3	0.3	118 ± 26	0.190 ± 0.005	–9.7 ± 0.8	Uni- and multilamellar

BNZ = benznidazole; SUV = small unilamellar vesicle.
* Percentage in weight of BNZ in relation to the total mass of membrane components.
† Size and *Z*-potential determined by dynamic light scattering.
‡ Morphological inspection by cryotransmission *electron* microscopy.

TABLE 3

Physicochemical characteristics (drug content, size distribution, and morphology) of the different samples of nanostructured cyclodextrins (CDs) loaded with benznidazole (BNZ) studied in the present work

		Particle size (μm)†			
Name	Drug* (%)	d(0.1)	d(0.5)	d(0.9)	Morphology‡/crystallinity§
CD 12	12	0.9 ± 1.5	7.4 ± 1.5	17.1 ± 2.0	Homogeneous nanostructure/ amorphous
CD 24	24	3.5 ± 0.4	9.5 ± 1.0	21.0 ± 2.2	Nanostructure + few non-nanostructured areas/mixture of amorphous and crystalline phases
CD 52	52	1.4 ± 0.1	7.2 ± 0.5	16.9 ± 1.1	Nanostructure + non-nanostructured areas/mixture of amorphous and crystalline phases
CD 48	48	1.5 ± 0.2	6.1 ± 0.3	13.7 ± 0.6	Nanostructure + non-nanostructured areas/mixture of amorphous and crystalline phases
CD 45	45	1.5 ± 0.3	8.1 ± 0.2	18.8 ± 0.6	Nanostructure + non-nanostructured areas/mixture of amorphous and crystalline phases

* Percentage in weight of BNZ in relation to the total mass of CD.
† Volumetric particle size distributions, measured by light scattering technique, d(0.1), d(0.5), and d(0.9), particle diameters (μm) under which there are 10%, 50%, and 90% of the total volume of the sample, respectively.
‡ Morphological inspection by scanning electron microscopy.
§ Crystallinity characterization by differential scanning calorimetry (DSC).

optimized with respect to both the number of cells per well and the detection time for each cell type. All tests were performed in triplicate and the experiments were run three times in different weeks. Medium and drug blanks were used in each test as controls. For the initial screening, the assays were performed at concentrations of 100, 10, and 1 μg nanoformulate/mL. L-929 and HepG2 cells were grown in MEM and Roswell Park Memorial Institute medium 1640, (Biochrom AG, Berlin, Germany), respectively, supplemented with 10% FBS. Cells from pre-confluent cultures were harvested with ethylenediaminetetraacetic acid–trypsin (Sigma-Aldrich and AppliChem) and maintained at 37°C in a humidified 5% CO_2 atmosphere. The L-929 and HepG2 cells were seeded in 96-well flat-bottom microplates (WWR Int LLC, Radnor, PA) (4×10^3 and 1.5×10^4 cells/well, respectively) and allowed to attach for 24 hours at 37°C. The medium was then replaced with medium containing different concentrations of drugs and the cells were incubated for another 24 hours. The cell proliferation reagent WST was added and the mixture incubated at 37°C for 3 hours. Measurements were performed with a scanning multi-well spectrophotometer (ELISA Multiskan reader, BioTek Instruments, Inc., Winooski, VT) at 450 nm wavelength. A second cytotoxicity assay using a wider range of nanoformulate concentrations was carried out to calculate the IC_{50} value (the drug concentration that inhibits the 50% of cell growth).

Epimastigote and trypomastigote/amastigote growth inhibition assays. In vitro biological activity assays were carried out using axenic cultures of *T. cruzi* (CL strain, clone B5) carrying *lacZ*,[39] generously provided by Gómez-Barrio.[40] Formulations with a low cytotoxicity for mammalian cells (< 20% inhibition)[41] were tested for their activity against epimastigotes chosen for preliminary screening because of its simple maintenance and relatively high drug sensitivity.[42] Drug activity was evaluated using the colorimetric method[43,44]. Absorbances and cell counts were compared to determine their correlation under the conditions of our laboratory. Epimastigotes were grown at 28°C in LIT containing 10% FBS and SP and harvested during the exponential growth phase (day 7). The screening assay was performed in 96-well microplates (WWR Int LLC) seeded with 2.5×10^5 epimastigotes/mL. After 72 hours of incubation at 28°C, the substrate chlorophenol red β-D-galactopyranoside (CPRG; Roche), prepared in 0.9% Triton X-100 solution (EMD, Darmstadt, Germany), was added to a final concentration of 200 μM. Once incubated at 37°C for an additional 3 hours, measurements at 595 nm wavelength were done. Efficacy was estimated by determining the epimastigote growth percentage (% EG value), calculated as follows: %EG = ([AE – AEB]/[AC – ACB] × 100), where AE is the absorbance of the

TABLE 4

Characterization (morphology, particle size, and zeta potential measurement) and properties of the different lipid nanoparticles (SLNs andNLCs)

Formulation	Drug (%)*	Size† (nm)	PDI‡	*Z* potential (mV)	EE (%)	Cumulative release (%)
SLN	0	261.96 ± 5.20	0.263 ± 0.02	–23.8 ± 0.66	–	–
	5	272.40 ± 7.95	0.232 ± 0.00	–23.7 ± 0.60	83.28	–
	10	265.20 ± 6.16	0.219 ± 0.02	–19.7 ± 0.05	88.68	–
	20	264.63 ± 5.04	0.262 ± 0.02	–23.1 ± 0.34	95.20	19.50
NLC	0	262.10 ± 4.03	0.371 ± 0.03	–23.0 ± 2.45	–	–
	5	389.20 ± 8.45	0.385 ± 0.01	–24.9 ± 1.17	98.81	–
	10	288.23 ± 43.01	0.447 ± 0.00	–27.3 ± 0.98	99.40	–
	20	273.73 ± 31.79	0.373 ± 0.01	–20.9 ± 1.15	99.69	38.30
	30	336.60 ± 20.87	0.384 ± 0.02	–29.8 ± 1.66	99.77	55.20

BNZ = benznidazole; EE = encapsulation efficiency; NLC = nanostructured lipid carrier; PDI = polydispersity index; SD = standard deviation; SLN = solid lipid nanoparticle.
* Percentage in weight of BNZ in relation to the total mass.
† Size: arithmetic mean values in nm ± SD.
‡ PDI: arithmetic mean values ± SD.

TABLE 5
Cytotoxicity of nine different SUVs preparations for cultured mammalian cells (L 929 and Hep G2)

	L 929			HepG2		
Formulate	100 μg/mL	10 μg/mL	1 μg/mL	100 μg/mL	10 μg/mL	1 μg/mL
QSa 0	95.5 ± 0.5	5.4 ± 4.8	8.9 ± 2.1	80.8 ± 0.3	13.1 ± 1.0	0.0 ± 0.0
QSb 0	88.5 ± 1.0	21.7 ± 4.1	2.1 ± 3.7	69.8 ± 3.3	25.3 ± 1.8	2.9 ± 5.0
QSc 0	83.3 ± 0.4	11.8 ± 2.5	5.9 ± 1.2	55.6 ± 4.0	4.5 ± 1.2	1.1 ± 0.2
QSd 0	82.4 ± 2.6	9.0 ± 2.6	0.9 ± 1.5	69.4 ± 0.7	10.6 ± 5.5	3.5 ± 2.8
LPa 0	2.6 ± 2.3	0.2 ± 0.4	0.0 ± 0.0	0.0 ± 0.0	0.0 ± 0.0	4.8 ± 3.1
LPc 0 (1)	39.4 ± 2.4	12.4 ± 2.8	3.2 ± 0.5	27.9 ± 5.7	0.0 ± 0.0	0.0 ± 0.0
LPc 0 (2)	32.1 ± 3.7	0.0 ± 0.0	0.0 ± 0.0	36.2 ± 4.9	4.0 ± 2.2	2.3 ± 2.4
LPb 0	0.0 ± 0.0	0.1 ± 0.17	0.0 ± 0.0	0.6 ± 1.1	0.0 ± 0.0	3.5 ± 4.7
LPb 0.3	0.0 ± 0.0	3.1 ± 3.2	14.9 ± 1.9	1.5 ± 2.6	0.0 ± 0.0	0.0 ± 0.0

ATCC = American Type Culture Collection; BNZ = benznidazole; SUV = small unilamellar vesicle; WST = water-soluble tetrazolium. Data reported as percentage of killed cells (WST test). QSa,b,c, and d: nonloaded quatsomes; LPa,c, and b 0: nonloaded liposomes; LPb 0,3: BNZ-loaded liposome; L 929: murine L-929 fibroblasts (NCTC clone 929); Hep G2: human liver hepatocellular cells ATCC.

experimental group, AEB the blank, AC the control group, and ACB the culture medium blank and free BNZ as reference.

To improve the specificity of the trypanocidal activity determination, compounds with low cytotoxicity (< 20% growth inhibition) and activity against epimastigotes greater than, or equal to free BNZ, were assayed against amastigotes. The assay was carried out in a tissue/cell culture system that allowed determining the activity against both amastigote and trypomastigote forms simultaneously. The lengthy of the assay (a full week) allows replication of intracellular *T. cruzi* amastigotes but also release of trypomastigotes. This obviously produces cultures in which the presence of a small proportion of trypomastigotes cannot be ruled out. This is the in vitro method of choice for screening drugs for their activity against *T. cruzi*,[41] because it mimics the lifecycle of the parasite in mammals since when treating patients both parasite forms will be coexisting.[45] TCD infective trypomastigotes were obtained from infected L-929 fibroblasts in MEMHSP. The assay was performed in 96-well microplates following the recommendations for drug screening.[41] Fibroblasts were seeded at a density of 4×10^3 cells/well in 80 μL of the abovedescribed medium, allowed to attach for 24 hours at 37°C, and then infected with 20 μL of TCD infective trypomastigotes/well in the same medium. The cell/parasite ratio was 1/10. After 2 hours of infection at 33°C, the medium, containing non-penetrated trypomastigotes, was discarded and replaced by 200 μL of MEM without phenol red supplemented with 10% FBS. After 48 hours, content of the wells was replaced by 200 μL of the dilutions of compounds in MEM without phenol red and incubated for 96 hours at 33°C. Fifty microliters of substrate (CPRG in 3% Triton X-100; final concentration 400 μM) was then added and measured at 595 nm wavelength after 24 hours at 37°C. Controls consisted of dimethyl sulfoxide 10%, fibroblasts, medium, drug, and untreated infected cells. The results were expressed as the percentage of viable *T. cruzi* in treated infected cells versus untreated infected cells: % AG = (AE – AEB)/(AC – ACB) × 100, where AE is the absorbance of the experimental group, AEB the compound (drug) blank, AC the absorbance of the control group (untreated infected cells), and ACB the culture medium (MEM) blank. The absorbance values of the uninfected fibroblasts were subtracted from the measurements. Free BNZ was used as the reference drug. Each concentration was tested in triplicate and each experiment was performed three times independently. The BNZ susceptibility of *T. cruzi* epimastigotes and trypomastigotes/amastigotes was determined and the IC_{50} (the drug concentration that eliminates 50% of the parasites) calculated (CL B5 strain IC_{50} to BNZ 14.9–26.8 μM) for each batch of formulates. An internal control of four BNZ concentrations, including the IC_{50}, was included in each plate. The selectivity index (SI) of each form of the parasite was calculated based on the ratio of the IC_{50} value in L-929 divided by the IC_{50} value of the parasite.[41]

Statistical analysis. All data are expressed as mean ± SE of the means (SEM). GraphPad Prism software was used to calculate the IC_{50} values. The significance was evaluated using Student's *t* test ($P < 0.05$ significant). In addition, the "*Z*-factor" was calculated (according to the formula $Z = 1 - (3 \text{ SD of sample} + 3 \text{ SD of control})/(\text{mean of the sample} - \text{mean of the control})$ to evaluate the quality of each in vitro assay.[46]

RESULTS AND DISCUSSION

Table 1 shows the membrane components of SUVs, their molar ratios, and total membrane components concentration. Table 2 shows the physicochemical characteristics of the different SUVs, BNZ unloaded and loaded. The ethanol content was below 200 ppm. All vesicular formulations have a

TABLE 6
Cytotoxicity of NLCs for mammalian cells (L 929 and Hep G2)

	L 929			HepG2		
Formulate	100 μg/mL	10 μg/mL	1 μg/mL	100 μg/mL	10 μg/mL	1 μg/mL
NLC O'	10.0 ± 1.6	5.6 ± 3.2	5.7 ± 5.4	9.5 ± 8.8	2.7 ± 4.7	2.4 ± 4.1
NLC 5′	5.0 ± 4.5	3.9 ± 3.7	3.7 ± 3.6	1.5 ± 2.7	0.3 ± 0.6	0.2 ± 0.1
NLC 10'	4.9 ± 4.3	3.2 ± 3.0	3.4 ± 3.6	1.2 ± 2.1	1.9 ± 1.6	5.4 ± 5.5
NLC 20''	5.3 ± 9.2	2.6 ± 4.4	2.2 ± 2.4	1.6 ± 0.8	0.5 ± 0.5	0.4 ± 0.5
NLC 30'	3.1 ± 1.8	0.3 ± 0.5	1.9 ± 3.3	4.9 ± 8.5	0.1 ± 0.1	0.7 ± 1.3

ATCC = American Type Culture Collection; Hep G2 = human liver hepatocarcinoma cells ATCC; L 929 = murine L-929 fibroblasts (NCTC clone 929); NLC = nanostructured lipid carriers; WST = water-soluble tetrazolium test. Data reported as percentage of killed cells (WST test).

TABLE 7
Cytotoxicity of nanostructured CD for mammalian cells (L 929 and Hep G2)

	L 929			HepG2		
Formulate	100 μg/mL	10 μg/mL	1 μg/mL	100 μg/mL	10 μg/mL	1 μg/mL
CD	3.4 ± 1	2.8 ± 3.1	3.4 ± 2.3	3.1 ± 3.1	3.8 ± 5.6	2.7 ± 3.6
CD 12	0 ± 0	0.8 ± 1.4	0.5 ± 0.9	0 ± 0	0.3 ± 0.6	0 ± 0
CD 24	1.0 ± 1.8	4.2 ± 7.2	1.8 ± 3.1	0 ± 0	0.4 ± 0.6	0.3 ± 0.3
CD 52	0.4 ± 0.8	1.7 ± 1.5	3.4 ± 3.0	0 ± 0	0.1 ± 0.2	0.4 ± 0.7

ATCC = American Type Culture Collection; CD = cyclodextrin; Hep G2 = human liver hepatocellular cells ATCC; L 929 = murine L-929 fibroblasts (NCTC clone 929); WST = water-soluble tetrazolium test. Data reported as percentage of killed cells (WST test).

mean diameter in the nanoscopic range. *Z*-potential values show that QSs were much more stable than LPs due to their high positive surface charges. *Z*-potential values of LPs were always below 30 mV, indicating that these formulations would sediment with time. However, in the case of LPs with polyethyleneglycol, this sedimentation is prevented through steric repulsion of PEG groups. Concerning CD, Table 3 shows the physicochemical characteristics of the different nanostructured CD complexes of BNZ. All CDs showed comparable size distribution, centered around 5–10 μm, when measured by light scattering. However, their structure at submicroscopic and supramolecular level was significantly heterogeneous as revealed by scanning electron microscopy and differential scanning calorimetry. Indeed, meanwhile sample CD 12 was completely amorphous and showed homogeneous nanostructure, crystalline and non-nanostructured areas were detected in the rest, whose extension increases with the BNZ loading. CD carried much more BNZ than LPs (Table 2) and were easily tuned by process parameters, major advantage of CD over SUVs.

The distribution of the loaded SLN particles before freeze-drying was monomodal (Table 4); the average particle size was ~166 nm and their *Z*-potential was –21 mV. The loaded NLCs were slightly larger, ~202 nm, with a *Z*-potential of –26.2 mV. The NLC formulations had an EE of ~99%, and the SLNs an EE of 95%. The cumulative release profiles of the loaded SLNs showed an initial burst of BNZ, reaching 18% at 1.5 hours for 20%. Thereafter, release was slower, such that the maximum BNZ release was 19.5%. The maximum release obtained with the BNZ-loaded NLCs was higher than that achieved with SLNs, although in this case the initial burst was reached 5 hours later.

TABLE 8
Nonspecific cytotoxicity of selected compounds for murine fibroblast (L 929)

	L 929	
Formulate	256 μM ± SD (*N* = 9)*	IC_{50} (μM)†
CD 12	24.2 ± 0.9	3367.7‡
CD 24	29.5 ± 0.1	2931.9‡
CD 52	31.5 ± 0.4	2284.9‡
CD 45	44.0 ± 2.2	1581.4‡
CD 48	39.1 ± 6.3	2446.9‡
NLC 20''	0 ± 0	1139.4
BNZ	3.9 ± 4.5	1436.9

BNZ = benznidazole; CD = cyclodextrin; L 929 = murine L-929 fibroblasts (NCTC clone 929); NLC = nanostructured lipid carriers; SD = standard deviation.

* The results are expressed as the mean value of nonspecific cytotoxicity (growth inhibition) at the highest concentration tested (256 μM) ± SD (*N* = 9 each).

† The concentration causing 50% growth inhibition was calculated using GraphPad Prism software.

‡ Significant differences ($P < 0.05$) compared with free BNZ (Student's *t* test).

Cytotoxicity. Empty QSs resulted to be toxic at high concentrations, although the reasons remain unknown.[47] In fact, toxicity was high for almost all preparations tested. The results pointed out that the cytotoxicity of QS was > 20%, which ruled out the use of these preparations. On the contrary, cytotoxicity of LPs was almost negligible; although BNZ-loaded LPs gave paradoxical results, since when assayed on fibroblasts, low concentrations exhibited marked toxicity (Table 5).

Unloaded lipid nanoparticles presented a concentration-dependent toxicity, whereas with the loaded nanoparticles, paradoxical results were obtained with a considerable degree of variability between replicates, warranting revision on the accuracy of the test in the evaluation of these particles. Based on both toxicity results and trypanocidal activity, we discard SLNs particles and keep on working with three new formulations of NLCs having faster initial burst. Toxicity was always < 15%. SEMs between experiments were actually high (Table 6). Similarly, WST tests for CD had an acceptable degree of cytotoxicity (< 20% growth inhibition), albeit with minor variations (Table 7). To calculate the SI, the cytotoxicity of the nanoformulates was determined over a broader range of concentrations (Table 8).

Biological activity: lipid nanoparticles SLN and NLC. SLN, NLC, and free BNZ had similar antiparasitic effect, which may be due to the kinetics of drug release from nanoparticles (Table 9). At the concentrations tested, IC_{50} values for the NLC 30% could not be measured since the values obtained were > 256 μM, the maximum concentration tested. NLC activities

TABLE 9
Biological activity of lipid SLNs and NLCs formulates against epimastigotes of *Trypanosoma cruzi* (CL strain, clone B5)

	Epimastigotes	
Formulate	256 μM ± SD (*N* = 9)*	IC_{50} (*N* = 9)†
SLN 5	40.7 ± 7.7	48.8 ± 14.3
SLN 10	28.5 ± 12.7	70.0 ± 17.
SLN 20	39.0 ± 2.3	123.9 ± 19.7
NLC 5	12.5 ± 2.1	93.9 ± 12.2
NLC 10	39.4 ± 2.8	119.8 ± 13.4
NLC 20	49.9 ± 3.1	256.0 ± 19.9
NLC 5′	31.6 ± 6.5	47.4 ± 17.7
NLC 10'	23.4 ± 0.9	41.3 ± 9.9
NLC 20'	24.2 ± 1.2	44.3 ± 7.5
NLC 30'	51.6 ± 1.2	Not feasible
NLC 20 ''	31.5 ± 1.1	53.9 ± 2.0
BNZ	15.8 ± 4.9	17.7 ± 2.1

BNZ = benznidazole; NLC = nanostructured lipid carriers; SD = standard deviation; SLN = solid lipid nanoparticles.

* The results are the mean value of epimastigote growth (%) at the highest concentration tested (256 μM) ± SD (*N* = 9).

† The concentration causing 50% cellular growth inhibition was calculated using GraphPad Prism software.

TABLE 10

Biological activity of CD formulates against epimastigotes of *Trypanosoma cruzi* (CL strain, clone B5)

Formulate	Epimastigotes	
	256 μM ± SD (N = 3)*	IC_{50} ± SD (N = 3)†
CD 12	19.0 ± 2.6	18.4 ± 4.7
BNZ	15.8 ± 4.9	14.8 ± 4.9

BNZ = benznidazole; CD = cyclodextrin; SD = standard deviation.

* The results are the mean values of epimastigote growth (%) at the highest concentration tested (256 μM) ± SD (N = 9).

† The concentration causing 50% cellular growth inhibition was calculated by using GraphPad Prism software.

improved when the particles were modified, although not enough to warrant further testing.

Liposomal and CD complexes. The BNZ concentrations reached in LPs (as low as < 12 μM) makes the antiparasitic effect negligible; thus, the IC_{50}determination was not feasible. However, the IC_{50} of the CD preparation (CD 12) was in the range of the IC_{50} of free BNZ; consistent with the enhanced solubility of the drug achieved with this formulation. Thus, CD 12 was further examined as a candidate antiparasitic agent (Table 10). CDs loaded with higher BNZ concentrations (CD 24 and CD 52) tend to form aggregates, making sonication of these particles mandatory in all experiments. The performances of the replicates, as determined by the susceptibility of *T. cruzi* strain CLB to the five CD–BNZ complexes and to free BNZ, are summarized in Table 11. A lower IC_{50} was obtained with sonicated CD 12 than with free BNZ. Among the formulations tested, the highest activities were achieved with CD 12 and CD 52 ($P < 0.05$, Student's t test).

To sum up, complexed CDs had a significantly lower toxicity than BNZ ($P < 0.05$, Student's t test). In their biological activity against the epimastigotes, NLC 20 were less effective than free BNZ (IC_{50} of 53.9 μM versus 26.8). The difference reflected the limited release of bounded BNZ. By contrast, loaded CDs had a similar activity against epimastigotes (16.7, 36.9, and 21.9 μM for CD 12, CD 24, and CD 52, respectively, versus 26.8 μM for free BNZ). It has been shown that CD favors the solubilisation of loaded molecules. In our case, this could be regarded as a reason to explain the results mentioned earlier.

The nanoparticles selected because of their low cytotoxicity and an antitrypanosomal activity higher than, or similar to, that of free BNZ were tested against the trypomastigote/amastigote form of the parasite. None of them had higher activity than BNZ. The least active lipid particles were NLC 20

TABLE 11

Biological activity of nanostructured CD formulates against epimastigotes of *Trypanosoma cruzi* (CL strain, clone B5) after sonication

Formulate	Epimastigotes	
	256 μM ± SD (N = 3)*	IC_{50} ± SD (N = 3)†
CD 12	26.9 ± 2.0	16.7 ± 4.6‡
CD 24	34.9 ± 3.2	36.9 ± 8.0
CD 52	33.0 ± 2.2	21.9 ± 1.2‡
CD 45	37.1 ± 1.2	46.7 ± 5.9
CD 48	37.9 ± 1.6	49.0 ± 2.5
BNZ	23.4 ± 0.9	26.8 ± 1.6

BNZ = benznidazole; CD = cyclodextrin; SD = standard deviation.

* The results are the mean values of epimastigote growth at the highest concentration tested (256 μM) ± SD (N = 3) in three independent experiments.

† The concentration causing 50% growth inhibition was calculated using GraphPad Prism software.

‡ Significant difference ($P < 0.05$) compared with free BNZ (Student's t test).

TABLE 12

Biological activity of nanostructured CD s and NLC 20'' against trypomastigotes/amastigotes of *Trypanosoma cruzi* (CL strain, clone B5)

Formulate	Trypomastigotes/amastigotes	
	256 μM ± SD (N = 9)*	IC_{50}†
CD 12	14.3 ± 0	4.0 ± 0
CD 24	21 ± 0.02	3.6 ± 1.6
CD 52	23.2 ± 0.05	5.2 ± 2.1
BNZ	16.9 ± 0.03	0.8 ± 0.4
NLC 20''	33.0 ± 0.02	17.6 ± 3.3

BNZ = benznidazole; CD = cyclodextrin; NLC = nanostructured lipid carriers; SD = standard deviation.

* The results are the mean trypomastigote/amastigote viability at the highest concentration tested (256 μM) ± SD (N = 3) in three independent experiments.

† The concentration causing 50% trypomastigote/amastigote growth inhibition was calculated using GraphPad Prism software.

(Table 12). Estimates of the SI of the nanoformulates leading to a parasite reduction similar to or higher than that of BNZ showed very high values in the cases of CD 12, CD 52, and CD 24 (Table 13). In all cases, the values were more than 50 what make them good candidates to be studied further (maximum tolerated dose in mice).[41] In vivo assays in mice are currently being performed. Experiments with CD-complexed BNZ effects on other discrete typing units of the parasite as recommended elsewhere[48] are being envisaged. Moreover, we are implementing new techniques by using image software to assess susceptibility of intracellular forms of the parasite.[49,50] In the in vitro assays, the Z-factor values ranged from 0.4 to 0.8, which demonstrated the feasibility of these experiments. The present work shows that the cytotoxicity of BNZ-loaded CDs was significantly lower than that of free BNZ without reduction in trypanocidal activity. This result should encourage further evaluations of CD 12-complexed BNZ as an improved therapeutic agent against Chagas disease. The differences in the activities of the nanoparticles against the two forms of the parasite raise questions regarding how antitrypanosomal agents reach their parasite target. Our work showed that the nanocomplexes were more active than free BNZ against the epimastigote stage, whereas higher nanoparticle doses were needed to reach intracellular forms.

CONCLUSIONS

In summary, BNZ should be regarded as an efficient trypanocidal, although it is toxic. SLN resulted to be less active than BNZ, whereas NLC were slightly less antitrypanosomal and more toxic than CD. Finally, among tested BNZ nanoformulates and nanocomplexes, CD gave the best-balanced antitrypanosomal/toxicity, whereas LPs resulted to be

TABLE 13

SI of benznidazole nanocomplexes

	Epimastigotes	Trypomastigotes
CD 12	199	836
CD 24	79	479
CD 52	104	522
CD 45	34	ND
CD 48	50	ND
NLC 20	21	69
BNZ	54	904

CD = cyclodextrin; ND = not done; SI = selectivity index. SI: ratio of the IC_{50} value in L-929 divided by the IC_{50} value of the parasite.

inadequate to carry and deliver BNZ, QS being too toxic (even more than free BNZ).

Received January 17, 2017. Accepted for publication June 2, 2017.

Published online October 2, 2017.

Note: Supplemental figure appears at www.ajtmh.org.

Acknowledgments: We thank the group of José A. Escario (Alicia Gomez-Barrio and Cristina Fonseca-Berzal) from the Parasitology Department of the Pharmacy Faculty of the University Complutense of Madrid, Spain, for providing us with the parasitic strains and for their valuable help. We also thank Eva Samanes and Maria Aguado for their help in the preparation of the Small unilamellar vesicles and the nanostructured cyclodextrin complexes. The copy-edition of the English manuscript by Wendy Ran is gratefully acknowledged.

Financial support: This article is part of the European project BERENICE. BERENICE is a Collaborative Project that is funded under the European Community's 7th Framework Programme. Grant agreement number: HEALTH-30593.

Disclosure: Miguel Viñas is member of the ENABLE (European Gram Negative Antibacterial Engine) European consortium (IMI-ND4BB, http://www.imi.europa.eu/content/enable).

Authors' addresses: Teresa Vinuesa, Rocio Herráez, Laura Oliver, and Miguel Viñas, Molecular Microbiology and Antimicrobials Laboratory, Department of Pathology and Experimental Therapeutics, Medical School, University of Barcelona, Barcelona, Spain, E-mails: tvinuesa@ub.edu, rhm1988@hotmail.com, laura.oliver.hernandez@gmail.com, and mvinyas@ub.edu. Elisa Elizondo, Nora Ventosa, and Jaume Veciana, Department of Molecular Nanoscience and Organic Materials, Institut de Ciència de Materials de Barcelona (ICMAB-CSIC), Cerdanyola del Vallès, Spain, E-mails: eelizondo@icmab.es, ventosa@icmab.es, and vecianaj@icmab.es. Argia Acarregui, Amaia Esquisabel, and Jose Luis Pedraz, Laboratory of Pharmaceutics, School of Pharmacy, University of the Basque Country (UPV/EHU), Vitoria, Spain, E-mails: argia_acarregui001@ehu.es, amaia.esquisabel@ehu.es, and joseluis.pedraz@ehu.es.

REFERENCES

1. Urbina JA, 2015. Recent clinical trials for the etiological treatment of chronic chagas disease: advances, challenges and perspectives. *J Eukaryot Microbiol 62:* 149–156.
2. Coura JR, Albajar Viñas P, 2010. Chagas disease: a new worldwide challenge. *Nature 465:* S6–S7.
3. Imai K, et al., 2014. Mother-to-child transmission of congenital Chagas disease, Japan. *Emerg Infect Dis 20:* 146–148.
4. World Health Organization, 2015. *Chagas Disease (American trypanosomiasis)*. Available at: http://www.who.int/mediacentre/factsheets/fs340/en/. Accessed.
5. Carlier Y, Sosa-Estani S, Luquetti AO, Buekens P, 2015. Congenital Chagas disease: an update. *Mem Inst Oswaldo Cruz 110:* 363–368.
6. Cruz OG, 1972 *Opera Omnia*. Rio de Janeiro, Brazil: Impressora Brasileira.
7. Lewis MD, Kelly JM, 2016. Putting infection dynamics at the heart of Chagas disease. *Trends Parasitol 32:* 899–911.
8. Viotti R, et al., 2014. Towards a paradigm shift in the treatment of chronic Chagas disease. *Antimicrob Agents Chemother 58:* 635–639.
9. Workman P, White RA, Walton MI, Owen LN, Twentyman PR, 1984. Preclinical pharmacokinetics of benznidazole. *Br J Cancer 50:* 291–303.
10. Morillo CA, et al., 2015. Randomized trial of benznidazole for chronic Chagas' cardiomyopathy. *N Engl J Med 373:* 1295–1306.
11. Molina I, Salvador F, Sánchez-Montalvá A, Treviño B, Serre N, Sao Avilés A, Almirante B, 2015. Toxic profile of benznidazole in patients with chronic Chagas disease: risk factors and comparison of the product from two different manufacturers. *Antimicrob Agents Chemother 59:* 6125–6131.
12. Pinazo MJ, Muñoz J, Posada E, López-Chejade P, Gállego M, Ayala E, Del Cacho E, Soy D, Gascon J, 2010. Tolerance of benznidazole in treatment of Chagas' disease in adults. *Antimicrob Agents Chemother 54:* 4896–4899.
13. González-Ramos J, Noguera-Morel L, Tong HY, Ramírez E, Ruiz-Bravo E, Bellón T, Cabañas R, Cachafeiro L, Herranz-Pinto P, 2016. Two cases of overlap severe cutaneous adverse reactions to benznidazole treatment for asymptomatic Chagas disease in a nonendemic country. *Br J Dermatol 175:* 604–607.
14. Bermudez J, Davies C, Simonazzi A, Pablo J, Palma S, 2016. Current drug therapy and pharmaceutical challenges for Chagas disease. *Acta Trop 156:* 1–16.
15. Molina I, et al., 2014. Randomized trial of posaconazole and benznidazole for chronic Chagas' disease. *N Engl J Med 370:* 1899–1908.
16. Francisco AF, Lewis MD, Jayawardhana S, Taylor MC, Chatelain E, Kelly JM, 2015. Limited ability of posaconazole to cure both acute and chronic *Trypanosoma cruzi* infections revealed by highly sensitive in vivo imaging. *Antimicrob Agents Chemother 59:* 4653–4661.
17. Coura JR, de Castro SL, 2002. A critical review on Chagas disease chemotherapy. *Mem Inst Oswaldo Cruz 97:* 3–24.
18. Molina J, Urbina J, Gref R, Brener Z, Rodrigues JM Jr, 2001. Cure of experimental Chagas' disease by the bis-triazole DO870 incorporated into "stealth" polyethyleneglycol-polylactide nanospheres. *J Antimicrob Chemother 47:* 101–104.
19. Morilla MJ, Benavidez P, Lopez MO, Bakas L, Romero EL, 2002. Development and in vitro characterisation of a benznidazole liposomal formulation. *Int J Pharm 249:* 89–99.
20. Silva JJN, Pavanelli WR, Salazar Gutierrez FR, Lima FCA, Da Silva ABF, Silva JS, Franco DW, 2008. Complexation of the anti-*Trypanosoma cruzi* drug benznidazole improves solubility and efficacy. *J Med Chem 51:* 4104–4114.
21. Morilla MJ, Prieto MJ, Romero EL, 2005. Benznidazole vs benznidazole in multilamellar liposomes: how different they interact with blood components? *Mem Inst Oswaldo Cruz 100:* 213–219.
22. Scalise ML, Arrua EC, Rial MS, Esteva MI, Salomon CJ, Fichera LE, 2016. Promising efficacy of benznidazole nanoparticles in acute *Trypanosoma cruzi* murine model: in-vitro and in-vivo studies. *Am J Trop Med Hyg 95:* 388–393.
23. Leonardi D, Salomón CJ, Lamas MC, Olivieri AC, 2009. Development of novel formulations for Chagas' disease: optimization of benznidazole chitosan microparticles based on artificial neural networks. *Int J Pharm 367:* 140–147.
24. Fonseca-Berzal C, Palmeiro-Roldán R, Escario JA, Torrado S, Arán VJ, Torrado-Santiago S, Gómez-Barrio A, 2015. Novel solid dispersions of benznidazole: preparation, dissolution profile and biological evaluation as alternative antichagasic drug delivery system. *Exp Parasitol 149:* 84–91.
25. Grillo R, Silva Melo NF, Moraes CM, Rosa AH, Frutuoso Roveda JA, Menezes CMS, Ferreira EI, Fraceto LF, 2007. Hydroxymethylnitrofurazone:dimethyl-β-cyclodextrin inclusion complex: a physical-chemistry characterization. *J Biol Phys 33:* 445–453.
26. Maximiano FP, Costa GHY, De Sá Barreto LCL, Bahia MT, Cunha-Filho MSS, 2011. Development of effervescent tablets containing benznidazole complexed with cyclodextrin. *J Pharm Pharmacol 63:* 786–793.
27. Lopes MS, Sales PA, Lopes AGF, Yoshida MI, da Silva THA, Romanha AJ, Alves RJ, de Oliveira RB, 2011. The activity of a metronidazole analogue and its β-cyclodextrin complex against *Trypanosoma cruzi*. *Mem Inst Oswaldo Cruz 106:* 1055–1057.
28. Lyra MAM, et al., 2012. Study of benznidazole–cyclodextrin inclusion complexes, cytotoxicity and trypanocidal activity. *J Incl Phenom Macrocycl Chem 73:* 397–404.
29. Leonardi D, Bombardiere ME, Salomon CJ, 2013. Effects of benznidazole:cyclodextrin complexes on the drug bioavailability upon oral administration to rats. *Int J Biol Macromol 62:* 543–548.
30. Nogueira D, Mitjans M, Rolim C, Vinardell M, 2014. Mechanisms underlying cytotoxicity induced by engineered nanomaterials: a review of in vitro studies. *Nanomaterials (Basel) 4:* 454–484.
31. Foldbjerg R, Wang J, Beer C, Thorsen K, Sutherland DS, Autrup H, 2013. Biological effects induced by BSA-stabilized silica

nanoparticles in mammalian cell lines. *Chem Biol Interact 204:* 28–38.
32. Buckner FS, 2011. Experimental chemotherapy and approaches to drug discovery for *Trypanosoma cruzi* infection. *Adv Parasitol 75:* 89–119.
33. Cabrera I, et al., 2013. Multifunctional nanovesicle-bioactive conjugates prepared by a one-step scalable method using CO_2-expanded solvents. *Nano Lett 13:* 3766–3774.
34. Elizondo E, Sala S, Imbuluzqueta E, González D, Blanco-Prieto MJ, Gamazo C, Ventosa N, Veciana J, 2011. High loading of gentamicin in bioadhesive PVM/MA nanostructured microparticles using compressed carbon-dioxide. *Pharm Res 28:* 309–321.
35. Cipolla D, Shekunov B, Blanchard J, Hickey A, 2014. Lipid-based carriers for pulmonary products: preclinical development and case studies in humans. *Adv Drug Deliv Rev 75:* 53–80.
36. Sans-Serramitjana E, Fusté E, Martínez-Garriga B, Merlos A, Pastor M, Pedraz JL, Esquisabel A, Bachiller D, Vinuesa T, Viñas M, 2016. Killing effect of nanoencapsulated colistin sulfate on *Pseudomonas aeruginosa* from cystic fibrosis patients. *J Cyst Fibros 15:* 611–618.
37. Lewinski N, Colvin V, Drezek R, 2008. Cytotoxicity of nanoparticles. *Small 4:* 26–49.
38. Guadagnini R, et al., 2015. Toxicity screenings of nanomaterials: challenges due to interference with assay processes and components of classic in vitro tests. *Nanotoxicology 9:* 13–24.
39. Buckner FS, Verlinde C, La Flamme AC, Van Voorhis WC, 1996. Efficient technique for screening drugs for activity against *Trypanosoma cruzi* using parasites expressing beta-galactosidase. *Antimicrob Agents Chemother 40:* 2592–2597.
40. Le-Senne A, Muelas-Serrano S, Fernández-Portillo C, Escario JA, Gómez-Barrio A, 2002. Biological characterization of a beta-galactosidase expressing clone of *Trypanosoma cruzi* CL strain. *Mem Inst Oswaldo Cruz 97:* 1101–1105.
41. Romanha AJ, et al., 2010. In vitro and in vivo experimental models for drug screening and development for Chagas disease. *Mem Inst Oswaldo Cruz 105:* 233–238.
42. Martinez Diaz RA, Escario JA, Nogal Ruiz JJ, Gomez Barrio A, 2000. Evaluation of drug activity against intracellular forms of *Trypanosoma cruzi* employing enzyme immunoassay. *J Clin Pharm Ther 25:* 43–47.
43. Vega C, Rolón M, Martínez-Fernández AR, Escario JA, Gómez-Barrio A, 2005. A new pharmacological screening assay with *Trypanosoma cruzi* epimastigotes expressing β-galactosidase. *Parasitol Res 95:* 296–298.
44. Fonseca-Berzal C, Merchán Arenas DR, Romero Bohórquez AR, Escario JA, Kouznetsov VV, Gómez-Barrio A, 2013. Selective activity of 2,4-diaryl-1,2,3,4-tetrahydroquinolines on *Trypanosoma cruzi* epimastigotes and amastigotes expressing β-galactosidase. *Bioorg Med Chem Lett 23:* 4851–4856.
45. Chatelain E, 2015. Chagas disease drug discovery: toward a new era. *J Biomol Screen 20:* 22–35.
46. Zhang JH, Chung TDOK, 1999. A simple statistical parameter for use in evaluation and validation of high throughput screening assays. *J Biomol Screen 4:* 67–73.
47. Hwang TL, Sung CT, Aljuffali IA, Chang YT, Fang JY, 2014. Cationic surfactants in the form of nanoparticles and micelles elicit different human neutrophil responses: a toxicological study. *Colloids Surf B Biointerfaces 114:* 334–341.
48. Zingales B, Miles MA, Moraes CB, Luquetti A, Guhl F, Schijman AG, Ribeiro I, 2014. Drug discovery for Chagas disease should consider *Trypanosoma cruzi* strain diversity. *Mem Inst Oswaldo Cruz 109:* 828–833.
49. Cal M, Ioset J-R, Fügi M, Mäser P, Kaiser M, 2016. Assessing anti-*T. cruzi* candidates in vitro for sterile cidality. *Int J Parasitol Drugs Drug Resist 6:* 165–170.
50. Yang G, Lee N, Ioset Jr NJ. 2016 Evaluation of parameters impacting drug susceptibility in intracellular *Trypanosoma cruzi* assay protocols. *SLAS Discov 22:* 125–134.

The following are supplemental materials and will be published online only

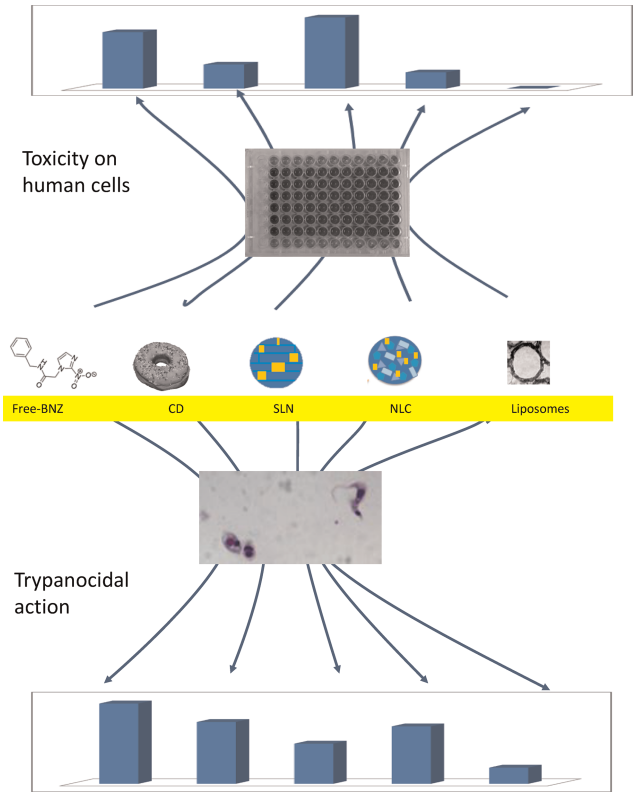

SUPPLEMENTAL FIGURE 1. Graphical abstract showing differences of toxicity on human cells and trypanosome parasites of benznidazol formulates tested.